

Solving conical diffraction grating problems with integral equations

Leonid I. Goray^{1,2,3,*} and Gunther Schmidt⁴

¹*I.I.G., Inc., P.O. Box 131611, Staten Island, New York 10313, USA*

²*Institute for Analytical Instrumentation, RAS, Rizhsky Prospect 26, St. Petersburg 190103, Russian Federation*

³*Saint Petersburg Academic University, Khlopina 8/3, St. Petersburg 194021, Russian Federation*

⁴*Weierstrass Institute of Applied Analysis and Stochastics, Mohrenstrasse 39, 10117 Berlin, Germany*

*Corresponding author: lig@pcgrate.com

Received October 5, 2009; accepted December 25, 2009;

posted January 19, 2010 (Doc. ID 118160); published February 25, 2010

Off-plane scattering of time-harmonic plane waves by a plane diffraction grating with arbitrary conductivity and general surface profile is considered in a rigorous electromagnetic formulation. Integral equations for conical diffraction are obtained involving, besides the boundary integrals of the single and double layer potentials, singular integrals, the tangential derivative of single-layer potentials. We derive an explicit formula for the calculation of the absorption in conical diffraction. Some rules that are expedient for the numerical implementation of the theory are presented. The efficiencies and polarization angles compared with those obtained by Lifeng Li for transmission and reflection gratings are in a good agreement. The code developed and tested is found to be accurate and efficient for solving off-plane diffraction problems including high-conductive gratings, surfaces with edges, real profiles, and gratings working at short wavelengths. © 2010 Optical Society of America

OCIS codes: 050.1950, 050.1960, 260.1960, 260.2110, 260.5430, 290.5820.

1. INTRODUCTION

Today a lot of optical applications of conical diffraction (off plane—see Fig. 1) by gratings are well known: in particular, gratings working in the x-ray and extreme ultraviolet ranges at grazing angles; shallow and deep high-conductive, anomalously absorbing gratings illuminated at near-normal and grazing incidence; high-spatial-frequency, deep transmission gratings having high antireflection and polarization conversion properties; and generalized spectroscopic ellipsometry and scatterometry techniques. For the numerical simulation of conical diffraction by optical gratings of arbitrary groove profiles and conductivity several rigorous methods have been proposed. Among them we know differential [1,2], coordinate transformation [3–6], modal [7], fictitious sources [8,9], and finite element [10,11] methods. In [12] T-matrix and integral equation methods (IMs) were described for off-plane transmission and low-conducting sine-profiled gratings.

For the classical (in-plane) diffraction problems boundary IMs have been established as an efficient and accurate numerical tool. The methods are used successfully to tackle high-conductive deep-groove gratings in the TM polarization, profile curves with corners, echelles, gratings with thin coated layers, randomly rough mirrors and gratings, and diffraction problems at very small wavelength-to-period ratios [13–22]. Many different integral formulations have been proposed and implemented; see, e.g., [22–30]. The aim of this paper is to study an integral method for conical diffraction on the simplest model, the diffraction of a time-harmonic plane wave by one surface, which in Cartesian coordinates (x, y, z) is pe-

riodic in the x - and invariant in the z -direction and separates two different materials. Special attention is paid to the main aspects of the IM for arbitrarily polarized plane waves and surface gratings having any outline and conductivity.

The electromagnetic formulation of the diffraction by general gratings, which are modeled as infinite periodic structures, can be reduced to a system of Helmholtz equations for the z components of the electric and magnetic fields in \mathbb{R}^2 , where the solutions have to be quasiperiodic in one variable, to be subject to radiation conditions with respect to the other, and to satisfy certain jump conditions at the interfaces between different materials of the diffraction grating. In the case of classical diffraction, when the incident wave vector is orthogonal to the z direction, the system splits into independent problems for the two basic polarizations of the incident wave, whereas for the case of conical diffraction the boundary values of the z components as well as their normal and tangential derivatives at the interfaces are coupled. Thus the unknowns are scalar functions in the case of classical diffraction, and they are two-component vector functions in the conical case.

In the considered case of one interface we reduce the system of Helmholtz equations to a 2×2 system of integral equations, which contain, besides the boundary integrals of the single- and double-layer potentials, additionally the tangential derivative of single-layer potentials, which are singular integrals. The corresponding theory is described in Section 2. The diffraction problem and boundary relations between values of the fields across the boundary are formulated in explicit form in Subsection

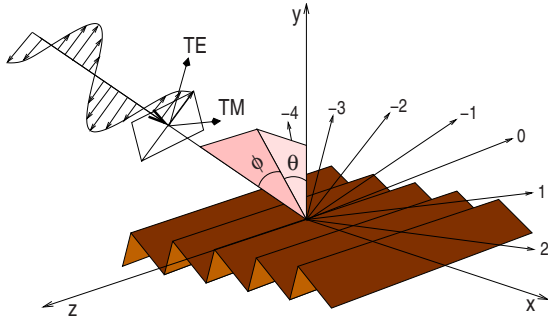


Fig. 1. (Color online) Schematic conical diffraction by a grating.

2.A. The respective integral equations in terms of boundary potentials with detailed discussions, formulas, and jump relations can be found in Subsection 2.B. A more general treatment of the energy conservation law applicable to off-plane absorption gratings is considered in Subsection 2.C. The numerical implementation approach expedient for the calculation of far fields and polarization properties of conical diffraction by gratings is described briefly in Section 3. Diverse numerical tests devoted to comparing, convergence, accuracy, computation time, and obtaining results for an important case are given in Section 4. In Subsection 4.A we compare some of our results with data obtained by other well-established conical approaches for different groove profile and conductivity gratings. Some information about convergence, accuracy, and complexity of the presented method is included in Subsection 4.B. Finally, in Subsection 4.C a numerical experiment for the off-plane grazing-incident real-groove-profile grating working in the soft-x-ray range is demonstrated as an illustration of possibilities of the software developed.

2. THEORY

A. Diffraction Problem

We denote by \mathbf{e}_x , \mathbf{e}_z , and \mathbf{e}_y the unit vectors of the axis of the Cartesian coordinates. The grating is a cylindrical surface whose generatrices are parallel to the z axis (see Fig. 1) and whose cross section is described by the curve Σ (Fig. 2). We suppose that Σ is not self-intersecting and d periodic in the x direction. The grating surface is the boundary between two regions $G_{\pm} \times \mathbb{R} \subset \mathbb{R}^3$, which are filled with materials of constant electric permittivity ϵ_{\pm} and magnetic permeability μ_{\pm} .

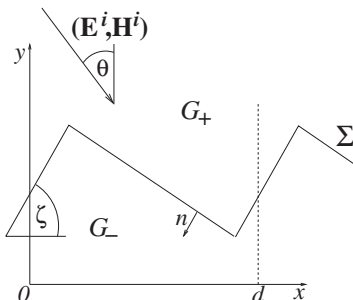


Fig. 2. Schematic diffraction by a simple grating in cross section.

We deal only with time-harmonic fields; consequently, the electric and magnetic fields are represented by the complex vectors \mathbf{E} and \mathbf{H} , with a time dependence $\exp(-i\omega t)$ taken into account. The wave vector \mathbf{k}_+ of the incident wave in $G_+ \times \mathbb{R}$, where $\epsilon_+, \mu_+ > 0$, is in general not perpendicular to the grooves ($\mathbf{k}_+ \cdot \mathbf{e}_z \neq 0$). Setting $\mathbf{k}_+ = (\alpha, -\beta, \gamma)$, the surface is illuminated by an electromagnetic plane wave

$$\mathbf{E}^i = \mathbf{p}e^{i(\alpha x - \beta y + \gamma z)}, \quad \mathbf{H}^i = \mathbf{s}e^{i(\alpha x - \beta y + \gamma z)},$$

which due to the periodicity of Σ is scattered into a finite number of plane waves in $G_+ \times \mathbb{R}$ and possibly in $G_- \times \mathbb{R}$. The wave vectors of these outgoing modes lie on the surface of a cone whose axis is parallel to the z axis. Therefore one speaks of conical diffraction.

The components of \mathbf{k}_+ satisfy

$$\beta > 0, \quad \alpha^2 + \beta^2 + \gamma^2 = \omega^2 \epsilon_+ \mu_+,$$

and they are expressed by using the incidence angles $|\theta|, |\phi| < \pi/2$:

$$(\alpha, -\beta, \gamma) = \omega \sqrt{\epsilon_+ \mu_+} (\sin \theta \cos \phi, -\cos \theta \cos \phi, \sin \phi).$$

Classical diffraction corresponds to $\mathbf{k}_+ \cdot \mathbf{e}_z = 0$, whereas $\phi \neq 0$ characterizes conical diffraction.

Since the geometry is invariant with respect to any translation parallel to the z axis, we make the ansatz for the total field

$$(\mathbf{E}, \mathbf{H})(x, y, z) = (E, H)(x, y)e^{i\gamma z}, \quad (1)$$

with $E, H: \mathbb{R}^2 \rightarrow \mathbb{C}^3$. This transforms the time-harmonic Maxwell equations in \mathbb{R}^3 ,

$$\nabla \times \mathbf{E} = i\omega \mu \mathbf{H}, \quad \nabla \times \mathbf{H} = -i\omega \epsilon \mathbf{E}, \quad (2)$$

with piecewise constant functions $\epsilon(x, y) = \epsilon_{\pm}$, $\mu(x, y) = \mu_{\pm}$ for $(x, y) \in G_{\pm}$, into a two-dimensional problem. This was described in [9] and analytically justified in [31]. Introducing the transverse components

$$E_T = E - E_z \mathbf{e}_z, \quad H_T = H - H_z \mathbf{e}_z,$$

representation (1) and Eqs. (2) lead to

$$(\omega^2 \epsilon \mu - \gamma^2) E_T = i\gamma \nabla E_z + i\omega \mu \nabla \times (H_z \mathbf{e}_z),$$

$$(\omega^2 \epsilon \mu - \gamma^2) H_T = i\gamma \nabla H_z - i\omega \epsilon \nabla \times (E_z \mathbf{e}_z). \quad (3)$$

Noting that $\gamma = \omega(\epsilon_+ \mu_+)^{1/2} \sin \phi$, we introduce the piecewise constant function

$$\kappa(x, y) = \begin{cases} (\epsilon_+ \mu_+ - \epsilon_+ \mu_+ \sin^2 \phi)^{1/2} = \kappa_+ & (x, y) \in G_+, \\ (\epsilon_- \mu_- - \epsilon_+ \mu_+ \sin^2 \phi)^{1/2} = \kappa_- & (x, y) \in G_-, \end{cases} \quad (4)$$

with the square root $z^{1/2} = r^{1/2} \exp(i\varphi/2)$ for $z = r \exp(i\varphi)$, $0 \leq \varphi < 2\pi$. Hence Eqs. (3) show that under the condition $\kappa \neq 0$, which will be assumed throughout, the components E_z, H_z determine the electromagnetic field (\mathbf{E}, \mathbf{H}) .

Additionally, Maxwell's equations (2) imply that E_z, H_z satisfy the Helmholtz equations

$$(\Delta + \omega^2 \kappa^2) E_z = (\Delta + \omega^2 \kappa^2) H_z = 0 \quad (5)$$

in G_{\pm} . The continuity of the tangential components of \mathbf{E} and \mathbf{H} on the surface takes the form

$$[(n, 0) \times E]_{\Sigma \times \mathbb{R}} = [(n, 0) \times H]_{\Sigma \times \mathbb{R}} = 0,$$

where $(n, 0) = (n_x, n_y, 0)$ is the normal vector on $\Sigma \times \mathbb{R}$ and $[(n, 0) \times E]_{\Sigma \times \mathbb{R}}$ denotes the jump of the function $(n, 0) \times E$ across the surface. This leads to the jump conditions for E_z, H_z across the interface Σ of the form

$$[E_z]_{\Sigma} = [H_z]_{\Sigma} = 0,$$

$$\left[\frac{\gamma}{\omega^2 \kappa^2} \partial_t H_z + \frac{\omega \epsilon}{\omega^2 \kappa^2} \partial_n E_z \right]_{\Sigma} = \left[\frac{\gamma}{\omega^2 \kappa^2} \partial_t E_z - \frac{\omega \mu}{\omega^2 \kappa^2} \partial_n H_z \right]_{\Sigma} = 0.$$

Here $\partial_n = n_x \partial_x + n_y \partial_y$ and $\partial_t = -n_y \partial_x + n_x \partial_y$ are the normal and tangential derivatives on Σ , respectively. We introduce $B_z = (\mu_+ / \epsilon_+)^{1/2} H_z$ and use $\gamma = \omega(\epsilon_+ \mu_+)^{1/2} \sin \phi$ to rewrite the jump conditions in the form

$$[E_z]_{\Sigma} = [H_z]_{\Sigma} = 0,$$

$$\left[\frac{\epsilon \partial_n E_z}{\kappa^2} \right]_{\Sigma} = -\epsilon_+ \sin \phi \left[\frac{\partial_t B_z}{\kappa^2} \right]_{\Sigma},$$

$$\left[\frac{\mu \partial_n B_z}{\kappa^2} \right]_{\Sigma} = \mu_+ \sin \phi \left[\frac{\partial_t E_z}{\kappa^2} \right]_{\Sigma}. \quad (6)$$

The z components of the incoming field

$$E_z^i(x, y) = p_z e^{i(\alpha x - \beta y)}, \quad B_z^i(x, y) = q_z e^{i(\alpha x - \beta y)}$$

$$\text{with } q_z = (\mu_+ / \epsilon_+)^{1/2} s_z, \quad (7)$$

are α quasiperiodic in x of period d , i.e., satisfy the relation

$$u(x + d, y) = e^{id\alpha} u(x, y).$$

In view of the periodicity of ϵ and μ , this motivates us to seek α -quasiperiodic solutions E_z, B_z . Furthermore, the diffracted fields must remain bounded at infinity, which implies the well-known outgoing wave conditions

$$(E_z, B_z)(x, y) = (E_z^i, B_z^i) + \sum_{n \in \mathbb{Z}} (E_n^+, B_n^+) e^{i(\alpha_n x + \beta_n^+ y)}, \quad y \geq H,$$

$$(E_z, B_z)(x, y) = \sum_{n \in \mathbb{Z}} (E_n^-, B_n^-) e^{i(\alpha_n x - \beta_n^- y)}, \quad y \leq -H, \quad (8)$$

with the unknown Rayleigh coefficients $E_n^{\pm}, H_n^{\pm} \in \mathbb{C}$, where $\Sigma \subset \{(x, y) : |y| < H\}$, and α_n, β_n^{\pm} are given by

$$\alpha_n = \alpha + \frac{2\pi n}{d}, \quad \beta_n^{\pm} = \sqrt{\omega^2 \kappa_{\pm}^2 - \alpha_n^2}$$

$$\text{with } 0 \leq \arg \beta_n^{\pm} < \pi.$$

In the following it is always assumed that

$$0 \leq \arg \epsilon_-, \quad \arg \mu_- \leq \pi \quad \text{with } \arg(\epsilon_- \mu_-) < 2\pi, \quad (9)$$

which holds for all existing optical (meta)materials. Then $0 \leq \arg \kappa_{\pm}^2 < 2\pi$ and β_n^{\pm} are properly defined for all n .

With the z components of the total fields denoted

$$E_z = \begin{cases} u_+ + E_z^i \\ u_- \end{cases}, \quad B_z = \begin{cases} v_+ + B_z^i & \text{in } G_+, \\ v_- & \text{in } G_-, \end{cases}$$

the problem of Eqs. (5), (6), and (8) can be written as

$$\Delta u_{\pm} + \omega^2 \kappa_{\pm}^2 u_{\pm} = \Delta v_{\pm} + \omega^2 \kappa_{\pm}^2 v_{\pm} = 0 \quad \text{in } G_{\pm}, \quad (10)$$

$$u_- = u_+ + E_z^i, \quad \frac{\epsilon_- \partial_n u_-}{\kappa_-^2} - \frac{\epsilon_+ \partial_n (u_+ + E_z^i)}{\kappa_+^2}$$

$$= \epsilon_+ \sin \phi \left(\frac{1}{\kappa_+^2} - \frac{1}{\kappa_-^2} \right) \partial_t v_- \quad \text{on } \Sigma,$$

$$v_- = v_+ + B_z^i, \quad \frac{\mu_- \partial_n v_-}{\kappa_-^2} - \frac{\mu_+ \partial_n (v_+ + B_z^i)}{\kappa_+^2}$$

$$= -\mu_+ \sin \phi \left(\frac{1}{\kappa_+^2} - \frac{1}{\kappa_-^2} \right) \partial_t u_- \quad \text{on } \Sigma, \quad (11)$$

$$(u_+, v_+)(x, y) = \sum_{n=-\infty}^{\infty} (E_n^+, B_n^+) e^{i(\alpha_n x + \beta_n^+ y)} \quad \text{for } y \geq H,$$

$$(u_-, v_-)(x, y) = \sum_{n=-\infty}^{\infty} (E_n^-, B_n^-) e^{i(\alpha_n x - \beta_n^- y)} \quad \text{for } y \leq -H. \quad (12)$$

B. Integral Equations

There exist different ways to transform the problem of Eqs. (10)–(12) to integral equations. We combine here the direct and indirect approaches as proposed in [23,24] for the case of classical diffraction. Let Σ be given by a piecewise C^2 parameterization

$$\sigma(t) = (X(t), Y(t)),$$

$$X(t+1) = X(t) + d,$$

$$Y(t+1) = Y(t), \quad t \in \mathbb{R}; \quad (13)$$

i.e., the continuous functions X, Y are piecewise C^2 and $\sigma(t_1) \neq \sigma(t_2)$ if $t_1 \neq t_2$. If the profile Σ has corners, then we suppose additionally that the angles between adjacent tangents at the corners are strictly between 0 and 2π .

The potentials that provide α -quasiperiodic solutions of the Helmholtz equation

$$\Delta u + k^2 u = 0 \quad \text{with } 0 \leq \arg k^2 < 2\pi \quad (14)$$

are based on the quasiperiodic fundamental solution of period d ,

$$\Psi_{k, \alpha}(P) = \lim_{N \rightarrow \infty} \frac{i}{2d} \sum_{n=-N}^N \frac{e^{i\alpha_n X + i\beta_n |Y|}}{\beta_n}, \quad P = (X, Y).$$

Here we assume that $\beta_n = (k^2 - \alpha_n^2)^{1/2} \neq 0$ for all n . The single- and double-layer potentials are defined by

$$\mathcal{S}\varphi(P) = 2 \int_{\Gamma} \varphi(Q) \Psi_{k, \alpha}(P - Q) d\sigma_Q,$$

$$\mathcal{D}\varphi(P) = 2 \int_{\Gamma} \varphi(Q) \partial_{n(Q)} \Psi_{k,\alpha}(P-Q) d\sigma_Q, \quad (15)$$

where Γ is one period of the interface Σ , i.e. $\Gamma = \{\sigma(t) : t \in [t_0, t_0 + 1]\}$ for some t_0 . In Eqs. (15) $d\sigma_Q$ denotes integration with respect to the arc length and $n(Q)$ is the normal to Σ at $Q \in \Sigma$ pointing into G_- . Obviously, for α -quasiperiodic densities φ on Σ the potentials $\mathcal{S}\varphi$, $\mathcal{D}\varphi$ are α -quasiperiodic in X and do not depend on the choice of Γ .

The potentials provide the usual representation formulas. Any α -quasiperiodic function u that satisfies in G_+ the Helmholtz equation (14) and the radiation condition

$$u(x,y) = \sum_{n=-\infty}^{\infty} u_n e^{i\alpha_n x + i\beta_n |y|}, \quad |y| \geq H,$$

admits the representation

$$\frac{1}{2}(\mathcal{S}\partial_n u - \mathcal{D}u) = \begin{cases} u & \text{in } G_+ \\ 0 & \text{in } G_- \end{cases}, \quad (16)$$

where the normal n points into G_- . Under the same assumptions for a function u in G_- the representation

$$\frac{1}{2}(\mathcal{D} - \mathcal{S}\partial_n u) = \begin{cases} 0 & \text{in } G_+ \\ u & \text{in } G_- \end{cases} \quad (17)$$

is valid.

Restriction of the potentials \mathcal{S} and \mathcal{D} to the profile curve Σ are the so-called boundary integral operators. The potentials provide the usual jump relations of classical potential theory. The single-layer potential is continuous across Σ :

$$(\mathcal{S}\varphi)^+(P) = (\mathcal{S}\varphi)^-(P) = V\varphi(P),$$

where the upper signs $+$ and $-$ denote the limits of the potentials for points in G_{\pm} tending in nontangential direction to $P \in \Sigma$, and V is a integral operator with logarithmic singularity

$$V\varphi(P) = 2 \int_{\Gamma} \Psi_{k,\alpha}(P-Q) \varphi(Q) d\sigma_Q, \quad P \in \Sigma.$$

The double-layer potential has a jump if crossing Γ :

$$(\mathcal{D}\varphi)^+ = (K - I)\varphi, \quad (\mathcal{D}\varphi)^- = (K + I)\varphi \quad (18)$$

with the boundary double-layer potential

$$K\varphi(P) = 2 \int_{\Gamma} \varphi(Q) \partial_{n(Q)} \Psi_{k,\alpha}(P-Q) d\sigma_Q + (\delta(P) - 1)\varphi(P).$$

Here $\delta(P) \in (0, 2)$, $P \in \Sigma$, denotes the ratio of the angle in G_+ at P and π , i.e., $\delta(P) = 1$ outside corner points of Σ . The normal derivative of $\mathcal{S}\varphi$ at Σ exists outside corners and has the limits

$$(\partial_n \mathcal{S}\varphi)^+ = (L + I)\varphi, \quad (\partial_n \mathcal{S}\varphi)^- = (L - I)\varphi, \quad (19)$$

where L is the integral operator on Γ with the kernel $\partial_{n(P)} \Psi_{k,\alpha}(P-Q)$,

$$L\varphi(P) = 2 \int_{\Gamma} \varphi(Q) \partial_{n(P)} \Psi_{k,\alpha}(P-Q) d\sigma_Q, \quad P \in \Sigma.$$

In the following the tangential derivative of single-layer potentials

$$\partial_t(V\varphi)(P) = 2\partial_t \int_{\Gamma} \Psi_{k,\alpha}(P-Q) \varphi(Q) d\sigma_Q, \quad P \in \Sigma,$$

also occurs. Interchanging differentiation and integration leads to an integral kernel with the nonintegrable main singularity

$$\frac{t(P) \cdot (P-Q)}{|P-Q|^2},$$

where $t(P)$ denotes the tangential vector to Σ at P . Therefore the tangential derivative of single-layer potentials cannot be expressed as a usual integral. But it can be interpreted as a Cauchy principal value or singular integral

$$J\varphi(P) = 2 \lim_{\delta \rightarrow 0} \int_{\Gamma \setminus \Gamma(P,\delta)} \varphi(Q) \partial_{t(P)} \Psi_{k,\alpha}(P-Q) d\sigma_Q = \partial_t(V\varphi)(P), \quad (20)$$

where $\Gamma(P, \delta)$ is the subarc of Γ of length 2δ with the midpoint P . Similarly, one can define the singular integral

$$H\varphi(P) = 2 \lim_{\delta \rightarrow 0} \int_{\Gamma \setminus \Gamma(P,\delta)} \varphi(Q) \partial_{t(Q)} \Psi_{k,\alpha}(P-Q) d\sigma_Q, \quad (21)$$

which by using integration by parts gives for α -quasiperiodic φ

$$H\varphi(P) = -2 \int_{\Gamma} \Psi_{k,\alpha}(P-Q) \partial_t \varphi(Q) d\sigma_Q = -V(\partial_t \varphi)(P), \quad P \in \Sigma.$$

Note that $V\partial_t V = VJ = -HV$.

Now we are in the position to formulate the integral equations for solving the conical diffraction problem (10)–(12). In order to represent u_{\pm} and v_{\pm} as layer potentials we assume in what follows that the parameters are such that $\beta_n^{\pm} = (\omega^2 \kappa_{\pm}^2 - \alpha_n^2)^{1/2} \neq 0$ for all n . Since $\arg \kappa_- \in [0, \pi]$ [see assumption (9)] the boundary integral operators corresponding to the fundamental solution $\Psi_{\omega\kappa_{\pm},\alpha}$ are well defined, and by Eqs. (16) and (17)

$$u_+ = \frac{1}{2}(\mathcal{S}^+ \partial_n u_+ - \mathcal{D}^+ u_+),$$

$$v_+ = \frac{1}{2}(\mathcal{S}^+ \partial_n v_+ - \mathcal{D}^+ v_+) \quad \text{in } G_+,$$

$$E_z^i = \frac{1}{2}(\mathcal{D}^+ E_z^i - \mathcal{S}^+ \partial_n E_z^i),$$

$$B_z^i = \frac{1}{2}(\mathcal{D}^+ B_z^i - \mathcal{S}^+ \partial_n B_z^i) \quad \text{in } G_-.$$

Here we denote by \mathcal{S}^{\pm} the single-layer potential defined on Γ with the fundamental solution $\Psi_{\omega\kappa_{\pm},\alpha}$. Correspondingly

D^\pm is the double-layer potential over Γ with the normal derivative of $\Psi_{\omega\kappa_\pm, \alpha}$ as kernel function. Taking the limits on Σ , the jump relations (18) lead to

$$\begin{aligned} V^+ \partial_n (u_+ + E_z^i) - (I + K^+)(u_+ + E_z^i) &= 2E_z^i|_\Sigma, \\ V^+ \partial_n (v_+ + B_z^i) - (I + K^+)(v_+ + B_z^i) &= 2B_z^i|_\Sigma, \end{aligned} \quad (22)$$

where V^\pm denote the boundary single-layer potentials

$$V^\pm \varphi(P) = 2 \int_\Gamma \varphi(Q) \Psi_{\omega\kappa_\pm, \alpha}(P - Q) d\sigma_Q, \quad P \in \Sigma,$$

and the operators K^\pm and L^\pm are defined analogously. The solutions in G_- are sought as single-layer potentials

$$u_- = S^- w, \quad v_- = S^- \tau$$

with certain auxiliary densities w, τ . Since by Eqs. (19)

$$\begin{aligned} u_-|_\Sigma &= V^- w, & \partial_n u_-|_\Sigma &= (L^- - I)w, \\ v_-|_\Sigma &= V^- \tau, & \partial_n v_-|_\Sigma &= (L^- - I)\tau, \end{aligned}$$

we see from Eqs. (22) that jump conditions (11) are valid when the unknowns w, τ satisfy the system of integral equations

$$\begin{aligned} \frac{\epsilon_- \kappa_+^2}{\epsilon_+ \kappa_-^2} V^+(L^- - I)w - (I + K^+)V^- w - \sin \phi \left(1 - \frac{\kappa_+^2}{\kappa_-^2}\right) V^+ \partial_t V^- \tau \\ = 2E_z^i, \\ \frac{\mu_- \kappa_+^2}{\mu_+ \kappa_-^2} V^+(L^- - I)\tau - (I + K^+)V^- \tau + \sin \phi \left(1 - \frac{\kappa_+^2}{\kappa_-^2}\right) V^+ \partial_t V^- w \\ = 2B_z^i. \end{aligned} \quad (23)$$

Recall that we assume $\kappa_\pm^2 \neq 0$ and $\omega^2 \kappa_\pm^2 - \alpha_n^2 \neq 0$ for all n .

For the analytical and numerical treatment of Eqs. (23) it is advantageous to use the relations

$$V^+ \partial_t V^- = -H^+ V^- = V^+ J^-$$

[see definitions (20) and (21)]. Then Eqs. (23) become a system of singular integral equations, for which powerful analytical and numerical methods exist.

If the solution of system (23) is found, then the solution of the conical diffraction problem Eqs. (10)–(12), can be determined by the relations

$$\begin{aligned} u_+ &= -\frac{1}{2} \left(\frac{\epsilon_- \kappa_+^2}{\epsilon_+ \kappa_-^2} S^+(I - L^-)w + D^+ V^- w \right. \\ &\quad \left. + \frac{\sin \phi (\kappa_-^2 - \kappa_+^2)}{\kappa_-^2} S^+ J^- \tau \right), \quad u_- = S^- w, \\ v_+ &= -\frac{1}{2} \left(\frac{\mu_- \kappa_+^2}{\mu_+ \kappa_-^2} S^+(I - L^-)\tau + D^+ V^- \tau \right. \\ &\quad \left. - \frac{\sin \phi (\kappa_-^2 - \kappa_+^2)}{\kappa_-^2} S^+ J^- w \right), \quad v_- = S^- \tau. \end{aligned}$$

A detailed mathematical analysis of system (23) is given in [32]. In particular, the following properties have been established:

1. The integral equations are equivalent to the Helmholtz system if the operators V^+ and V^- are invertible.
2. If the profile Σ has no corners, then Eqs. (23) are solvable if $\epsilon_- + \epsilon_+ \neq 0$ and $\mu_- + \mu_+ \neq 0$.
3. If the profile Σ has corners, then Eqs. (23) are solvable if ϵ_- / ϵ_+ and $\mu_- / \mu_+ \notin [-\rho, -1/\rho]$ for some $\rho > 1$, depending on the angles at these corners.
4. The solution of Eqs. (23) is unique if $\text{Im } \epsilon_- \geq 0$ and $\text{Im } \mu_- \geq 0$ with $\text{Im}(\epsilon_- + \mu_-) > 0$.

C. Energy Balance for Conical Diffraction

Suppose that E_z, B_z are a solution of the partial differential formulation of conical diffraction, Eqs. (5), (6), and (8). The expression of the conservation of energy can be derived from a variational equality for E_z and B_z in a periodic cell Ω_H , which has in the x direction the width d , is bounded by the straight lines $\{y = \pm H\}$, and contains Γ . We multiply Eq. (5) by

$$\frac{\epsilon}{\epsilon_+ \kappa_+^2} \overline{E_z}, \quad \frac{\mu}{\mu_+ \kappa_+^2} \overline{B_z}$$

and apply Green's formula in the subdomains $\Omega_H \cap G_\pm$. Then, by using the quasiperiodicity of E_z, B_z and jump relations (6), one derives

$$\begin{aligned} \int_{\Omega_H} \frac{\epsilon}{\epsilon_+} \left(\frac{1}{\kappa_+^2} |\nabla E_z|^2 - \omega^2 |E_z|^2 \right) + \sin \phi \left(\frac{1}{\kappa_+^2} - \frac{1}{\kappa_-^2} \right) \int_\Gamma \partial_t B_z \overline{E_z} \\ - \frac{1}{\kappa_+^2} \int_{\Gamma(H)} \partial_n E_z \overline{E_z} - \frac{\epsilon_-}{\epsilon_+ \kappa_-^2} \int_{\Gamma(-H)} \partial_n E_z \overline{E_z} = 0, \end{aligned} \quad (24)$$

$$\begin{aligned} \int_{\Omega_H} \frac{\mu}{\mu_+} \left(\frac{1}{\kappa_+^2} |\nabla B_z|^2 - \omega^2 |B_z|^2 \right) - \sin \phi \left(\frac{1}{\kappa_+^2} - \frac{1}{\kappa_-^2} \right) \int_\Gamma \partial_t E_z \overline{B_z} \\ - \frac{1}{\kappa_+^2} \int_{\Gamma(H)} \partial_n B_z \overline{B_z} - \frac{\mu_-}{\mu_+ \kappa_-^2} \int_{\Gamma(-H)} \partial_n B_z \overline{B_z} = 0, \end{aligned} \quad (25)$$

where $\Gamma(\pm H)$ denotes the upper and the lower straight boundary of Ω_H , respectively, and the normal n on $\Gamma(\pm H)$ is directed outward. The outgoing wave conditions (8) imply

$$\begin{aligned} \int_{\Gamma(H)} \partial_n E_z \overline{E_z} &= i\beta(|E_0^+|^2 - |p_z|^2) + 2i \text{Im}(E_0^+ \overline{p_z} e^{i\beta H}) \\ &\quad + i \sum_{n \neq 0} \beta_n^+ |E_n^+|^2 e^{-2H \text{Im } \beta_n^+}, \\ \int_{\Gamma(-H)} \partial_n E_z \overline{E_z} &= i \sum_{n \in \mathbb{Z}} \beta_n^- |E_n^-|^2 e^{-2H \text{Im } \beta_n^-}, \end{aligned}$$

and similar expressions for the boundary integrals involving B_z .

Note that ϵ_+ and μ_+ are positive, and let ϵ_- and μ_- be real. Taking the imaginary part of Eqs. (24) and (25), one gets

$$\begin{aligned} & \frac{\beta}{\kappa_+^2} |p_z|^2 - \frac{1}{\kappa_+^2} \sum_{\beta_n^+ > 0} \beta_n^+ |E_n^+|^2 - \frac{\epsilon_-}{\epsilon_+ \kappa_-^2} \sum_{\beta_n^- > 0} \beta_n^- |E_n^-|^2 \\ &= -\sin \phi \left(\frac{1}{\kappa_+^2} - \frac{1}{\kappa_-^2} \right) \text{Im} \int_{\Gamma} \partial_t B_z \overline{E_z}, \end{aligned}$$

$$\begin{aligned} & \frac{\beta}{\kappa_+^2} |q_z|^2 - \frac{1}{\kappa_+^2} \sum_{\beta_n^+ > 0} \beta_n^+ |B_n^+|^2 - \frac{\mu_-}{\mu_+ \kappa_-^2} \sum_{\beta_n^- > 0} \beta_n^- |B_n^-|^2 \\ &= \sin \phi \left(\frac{1}{\kappa_+^2} - \frac{1}{\kappa_-^2} \right) \text{Im} \int_{\Gamma} \partial_t E_z \overline{B_z}, \end{aligned}$$

which in view of

$$\text{Im} \int_{\Gamma} \partial_t B_z \overline{E_z} = \text{Im} \int_{\Gamma} \partial_t E_z \overline{B_z}$$

lead to

$$\begin{aligned} |p_z|^2 + |q_z|^2 &= \sum_{\beta_n^+ > 0} \frac{\beta_n^+}{\beta} (|E_n^+|^2 + |B_n^+|^2) \\ &+ \frac{\kappa_+^2}{\kappa_-^2} \sum_{\beta_n^- > 0} \frac{\beta_n^-}{\beta} \left(\frac{\epsilon_-}{\epsilon_+} |E_n^-|^2 + \frac{\mu_-}{\mu_+} |B_n^-|^2 \right). \end{aligned}$$

Thus, for lossless gratings, the energy of the incident wave $|p_z|^2 + |q_z|^2$ equals the sum of reflection order efficiencies

$$R = \sum_{\beta_n^+ > 0} \frac{\beta_n^+}{\beta} (|E_n^+|^2 + |B_n^+|^2)$$

plus the sum of transmission order efficiencies

$$T = \sum_{\beta_n^- > 0} \frac{\beta_n^-}{\beta} \left(\frac{\epsilon_-}{\epsilon_+} |E_n^-|^2 + \frac{\mu_-}{\mu_+} |B_n^-|^2 \right).$$

If $\text{Im} \epsilon_- \neq 0$ or $\text{Im} \mu_- \neq 0$, then $T=0$ and in general $|p_z|^2 + |q_z|^2 > R$. The remaining part of the energy is absorbed in the substrate. Therefore, one tool to check the quality of the numerical solution for absorbing gratings is the requirement that the sum of the reflected energy and the absorption energy should be equal to the energy of the incident wave.

To obtain an expression for the absorption energy we apply Green's formula to E_z and B_z in the domain $\Omega_H \cap G_-$, which gives, since the normal n on Γ is interior for $\Omega_H \cap G_-$,

$$\begin{aligned} & \int_{\Omega_H \cap G_-} \frac{\epsilon_-}{\epsilon_+} \left(\frac{1}{\kappa_-^2} |\nabla E_z|^2 - \omega^2 |E_z|^2 \right) - \frac{\epsilon_-}{\epsilon_+ \kappa_-^2} \int_{\Gamma(-H)} \partial_n E_z \overline{E_z} \\ &= -\frac{\epsilon_-}{\epsilon_+ \kappa_-^2} \int_{\Gamma} \partial_n E_z \overline{E_z}, \end{aligned}$$

$$\begin{aligned} & \int_{\Omega_H \cap G_-} \frac{\mu_-}{\mu_+} \left(\frac{1}{\kappa_-^2} |\nabla B_z|^2 - \omega^2 |B_z|^2 \right) - \frac{\mu_-}{\mu_+ \kappa_-^2} \int_{\Gamma(-H)} \partial_n B_z \overline{B_z} \\ &= -\frac{\mu_-}{\mu_+ \kappa_-^2} \int_{\Gamma} \partial_n B_z \overline{B_z}. \end{aligned}$$

Hence, the imaginary parts of Eqs. (24) and (25) become

$$\begin{aligned} & \text{Im} \frac{\epsilon_-}{\epsilon_+ \kappa_-^2} \int_{\Gamma} \partial_n E_z \overline{E_z} - \sin \phi \text{Im} \left(\frac{1}{\kappa_+^2} - \frac{1}{\kappa_-^2} \right) \int_{\Gamma} \partial_t B_z \overline{E_z} \\ &+ \frac{\beta}{\kappa_+^2} (|E_0^+|^2 - |p_z|^2) + \sum_{\beta_n^+ > 0} \frac{\beta_n^+}{\kappa_+^2} |E_n^+|^2 = 0, \end{aligned}$$

$$\begin{aligned} & \text{Im} \frac{\mu_-}{\mu_+ \kappa_-^2} \int_{\Gamma} \partial_n B_z \overline{B_z} + \sin \phi \text{Im} \left(\frac{1}{\kappa_+^2} - \frac{1}{\kappa_-^2} \right) \int_{\Gamma} \partial_t E_z \overline{B_z} \\ &+ \frac{\beta}{\kappa_+^2} (|B_0^+|^2 - |q_z|^2) + \sum_{\beta_n^+ > 0} \frac{\beta_n^+}{\kappa_+^2} |B_n^+|^2 = 0, \end{aligned}$$

resulting in

$$\begin{aligned} |p_z|^2 + |q_z|^2 &= \sum_{\beta_n^+ > 0} \frac{\beta_n^+}{\beta} (|E_n^+|^2 + |B_n^+|^2) + \text{Im} \frac{\epsilon_- \kappa_+^2}{\epsilon_+ \kappa_-^2 \beta} \int_{\Gamma} \partial_n E_z \overline{E_z} \\ &+ \text{Im} \frac{\mu_- \kappa_+^2}{\mu_+ \kappa_-^2 \beta} \int_{\Gamma} \partial_n B_z \overline{B_z} - \frac{\sin \phi}{\beta} \\ &\times \left(\text{Im} \left(1 - \frac{\kappa_+^2}{\kappa_-^2} \right) \int_{\Gamma} (\partial_t B_z \overline{E_z} - \partial_t E_z \overline{B_z}) \right) \\ &= \sum_{\beta_n^+ > 0} \frac{\beta_n^+}{\beta} (|E_n^+|^2 + |B_n^+|^2) + \frac{\kappa_+^2}{\beta} \text{Im} \int_{\Gamma} \left(\frac{\epsilon_-}{\epsilon_+ \kappa_-^2} \partial_n E_z \overline{E_z} \right. \\ &+ \left. \frac{\mu_-}{\mu_+ \kappa_-^2} \partial_n B_z \overline{B_z} \right) \\ &+ \frac{2\kappa_+^2 \sin \phi}{\beta} \text{Im} \frac{1}{\kappa_-^2} \text{Re} \int_{\Gamma} E_z \partial_t \overline{B_z}. \end{aligned}$$

Thus we derive the conservation of energy for absorbing gratings

$$|p_z|^2 + |q_z|^2 = R + A$$

with the absorption energy of conical diffraction

$$\begin{aligned} A &= \frac{\kappa_+^2}{\beta} \text{Im} \left(\frac{1}{\kappa_-^2} \left(\frac{\epsilon_-}{\epsilon_+} \int_{\Gamma} \partial_n E_z \overline{E_z} + \frac{\mu_-}{\mu_+} \int_{\Gamma} \partial_n B_z \overline{B_z} \right. \right. \\ &+ \left. \left. 2 \sin \phi \text{Re} \int_{\Gamma} E_z \partial_t \overline{B_z} \right) \right). \end{aligned}$$

In the case $\phi=0$ this formula provides the expression of the heat absorption energy for in-plane diffraction derived in [21]. In terms of the solution w, τ of integral equations (23) the absorption energy is given by the formula

$$A = \frac{\kappa_+^2}{\beta} \operatorname{Im} \left(\frac{1}{\kappa_-^2} \int_{\Gamma} \left(\frac{\epsilon_-}{\epsilon_+} (L^- - I) w \overline{V^- w} + \frac{\mu_-}{\mu_+} (L^- - I) \tau \overline{V^- \tau} \right) \right) + \frac{2\kappa_+^2 \sin \phi}{\beta} \operatorname{Im} \frac{1}{\kappa_-^2} \operatorname{Re} \int_{\Gamma} V^- w \overline{J^- \tau}. \quad (26)$$

3. NUMERICAL IMPLEMENTATION

We discuss briefly the numerical solution of system (23). Let Γ be parameterized by Eqs. (13). In the case of a smooth profile Σ a trigonometric collocation method is used; i.e., we approximate

$$w(\sigma(t)) e^{-i\alpha X(t)} |\sigma'(t)| \approx w_N(t) = \sum_{k=-N}^N a_k e^{2\pi i k t},$$

$$\tau(\sigma(t)) e^{-i\alpha X(t)} |\sigma'(t)| \approx \tau_N(t) = \sum_{k=-N}^N b_k e^{2\pi i k t}, \quad (27)$$

and the coefficients $\{a_k\}, \{b_k\}$ are such that system (23) is satisfied at the $2N+1$ collocation points $t_k = k/(2N+1)$, $k = 0, \dots, 2N$.

Similar to [24], the advantage of trigonometric methods is utilized in order that the integral operators V^\pm, H^\pm , and J^\pm with singular kernels can be approximated properly. For example, using the parameterization $\sigma(t)$ the single-layer potential operator of w can be approximated by

$$V^\pm w(\sigma(t)) \approx -2e^{i\alpha X(t)} \left(\int_0^1 \log|2 \sin \pi(t-s)| w_N(s) ds + \int_0^1 g^\pm(t,s) w_N(s) ds \right)$$

and the singular integral $J^\pm w$ by

$$J^\pm w(\sigma(t)) \approx e^{i\alpha X(t)} \left(\int_0^1 \cot \pi(t-s) w_N(s) ds + \int_0^1 j^\pm(t,s) w_N(s) ds \right),$$

where the functions $g^\pm(t,s), j^\pm(t,s)$ are continuous and periodic in t and s . The action of the integral operators with the kernels $\log|2 \sin \pi(t-s)|$ and $\cot \pi(t-s)$ on trigonometric polynomials is given analytically. All other integrals have continuous kernels, and they are approximated by the trapezoidal rule as in Nyström's method. So the discretization error depends only on the error made in computing the functions $g^\pm(t,s), j^\pm(t,s)$ and the continuous kernels of K^+ and L^- , i.e., in computing the fundamental solution and their derivatives. Here we use the exact Ewald method (see [22]) with a number of summation terms to ensure discretization errors of order N^{-3} . Finally the operator products $V^+L^-, K^+V^-, H^+V^-,$ or V^+J^- are ap-

proximated by the products of the corresponding discretization matrices. Note that instead of H^+V^- or V^+J^- one can also perform the discretization of $V^+\partial_t V^-$, involving a numerical differentiation. Numerical tests and further investigations can show which one is preferable for given efficiency calculations.

For the solution of the discrete system we use a preconditioned generalized minimal residual method similar to that described in [22]. The number of iterations until a prescribed residual error is reached depends, of course, on the refraction indices and the profile, but it is nearly independent of the number of unknowns. However, it should be noted that modern implementations of the LAPACK and BLAS software packages on multiprocessor machines make direct solving a competitive alternative to iterative solution methods even for rather large systems.

If the profile curve has corners, then the convergence properties of methods with only trigonometric trial functions deteriorate owing to singularities of the densities w and τ of the form $O(\rho^{-\delta})$, $0 < \delta < 1$, where ρ is the distance to the closest edge. In boundary element methods it is common to use piecewise polynomial trial functions on meshes graded toward corner points. But because of the complicated form of their kernels the quadrature of the integral operators acting on piecewise polynomials is very expensive. Therefore we use a modification of the trigonometric collocation scheme with a fixed number of piecewise polynomial trial functions. First we introduce meshes of collocation points, which contain the corners and are graded toward the corner points. This can be derived by changing parameterization (13); for example, if $\sigma(t_j)$ is a corner point, then $\sigma'(t_j) = \sigma''(t_j) = 0$ implies grading toward the corner. Further, for each collocation point t_k there exists a Lagrangian trigonometric polynomial $p_k(t)$ of degree $2N+1$ such that

$$p_k(t_j) = \delta_{kj}, \quad k, j = 0, \dots, 2N,$$

where δ_{kj} is Kronecker's delta. For each edge and a fixed number of collocation points t_k around it, we replace the corresponding Lagrangian trigonometric polynomial $p_k(t)$ by a cubic spline $s_k(t)$ on the graded mesh with $s_k(t_j) = \delta_{kj}$. Thus we get a hybrid trigonometric-spline collocation method, which combines the efficient computation of the integrals for trigonometric polynomials with the good approximation properties of piecewise polynomials on graded meshes near edges. The values at the collocation point t_j of the integrals on the basis spline s_k are computed by a composite Gauss quadrature with a quadrature mesh geometrically graded toward t_j and depending on the distance $|\sigma(t_k) - \sigma(t_j)|$. This leads to a fixed number of additional calculations of the fundamental solutions $\Psi_{\omega\kappa_\pm, \alpha}$ for each discretization level compared with the pure trigonometric method, which is, however, compensated by a significant higher accuracy.

4. NUMERICAL RESULTS

The workability of the code developed has been confirmed by numerous tests usually employed in classical and conical diffraction cases: more specifically, the reciprocity theorem; stabilization of results under doubling of the number of collocation points and varying of the calcula-

tion accuracy of kernel functions; comparison with analytically amenable cases of plane interfaces; consideration of the inverse (nonphysical) radiation condition; use of different variants of collocation point distribution on boundaries (mesh refinements); and comparison with the results obtained by another of our codes or with published data, or with information sent to us by other researchers, including results of measurements. A small part of such numerical tests is demonstrated in this section.

A. Comparison

In Table 1 the numerical results of the present IM for a dielectric lamellar grating with the ridge width c and depth $2H$ in a conical mounting are compared with those of Table 2 of Li, who uses the modal method (MM) [33]. All grating and light parameters are listed in the table title. The agreement between the MM and the IM for the efficiencies and polarization angles is almost perfect for all reflection and transmission orders despite the very different methods compared. Note that we use the same definitions for polarization angles δ and ψ as in [30,33]. We used 400 collocation points, mesh grading, and the direct discretization of J^- to calculate this example that allocates 188 Mbytes of memory. The energy balance error calculated from Eq. (26) is $\sim 10^{-5}$. The average time taken up by the example on a portable workstation IBM ThinkPad R50p with an Intel Pentium M 1.7 GHz processor and 2 Gbytes of RAM is ~ 4 s when operating on Linux (kernel 2.6.17).

In Table 2 the numerical results of a comparison similar to that in Table 1 between the IM and the MM are demonstrated for a conducting lamellar grating in a conical mounting (compare Table 3 of [33]). All grating and light parameters are listed in the table title. The agreement between the MM and the IM for the efficiencies and polarization angles is, in general, good. The same accuracy parameters as in the previous example have been used, and similar calculation times have been obtained on the above-mentioned laptop. The energy balance error calculated from Eq. (26) is $\sim 10^{-6}$.

In Tables 3 and 4 the numerical results of the IM for a dielectric sine grating in a conical mounting are compared with those of Table 2 of [7] of Li, who used for the presented data the coordinate transformation method (CM) [5]. All grating and light parameters are listed in the table titles. The agreement between the CM and the IM

for the efficiencies is very good. We used 100 collocation points and the numerical differentiation of V^+ to calculate this example, which allocates 10 Mbytes of RAM. The energy balance error calculated from Eq. (26) is about 10^{-5} for both components of the incident radiation. The average computation time taken up by the example on the above mentioned laptop is ~ 0.2 s.

The results for a metal echelette grating with the blaze angle ζ and an apex angle of 90° (see Fig. 2) in conical mounting are compared in Tables 5 and 6 with those of [34] updated by Li, who has again used the CM to calculate the efficiency of the grating with edges [35]. All grating and light parameters are listed in the table titles. As one can see in Tables 5 and 6, again the agreement between the CM and the IM is very good for all order efficiencies and polarization angles. We have used 800 collocation points, mesh scaling near edges, and the differentiation of V^+ to calculate this example, allocating 196 Mbytes of RAM. The average energy balance error calculated from Eq. (26) is $\sim 10^{-5}$ for both polarization states of the incident radiation. The average computation time taken up by two values of the polarization angle on the above mentioned laptop is ~ 18 s.

B. Convergence, Accuracy, and Computation Time

We will examine the convergence rate and the accuracy of diffraction efficiencies with respect to the number of collocation points N . For the efficiency convergence testing, a magnitude of computational error cannot be reliably deduced from accuracy criteria based on a single computation such as the energy balance or the inverse radiation condition tests. For this purpose comparative studies should be used, i.e., N doubling or changing the configuration of collocation points. We introduce a parameter $\Delta_{N,k}$ as an integral measure of the efficiency error under N -doubling tests. It is equal to the sum of absolute differences of respective diffraction order efficiencies for two successive iterations with the number of collocation points for each iteration of $N=N_0 \times 2^{k-1}$, where N_0 is the initial number of collocation points, $k=1, \dots, K$, and K is the total number of iterations. The magnitude of $\Delta_{N,k}$ gives approximately the correct digits in the numerical results if the number of propagating diffraction orders is small enough or only a few valuable orders exist. For many propagating orders it can give a more pessimistic error value.

Table 1. Diffraction Angles (θ , ϕ), Diffraction Efficiencies (η), and Polarization Angles (δ , ψ) of a Dielectric Lamellar Grating^a

DO ^b	θ (IM), deg	ϕ (IM), deg	η (MM), %	η (IM), %	δ (MM), deg	δ (IM), deg	ψ (MM), deg	ψ (IM), deg
R_{-2}	35.265	-30	0.1614	0.1612	64.32	64.32	-30.30	-30.24
R_{-1}	0	-30	0.3807	0.3807	65.97	66.0	-157.20	-157.22
R_0	35.264	-30	1.855	1.854	70.49	70.43	-148.46	-148.60
T_{-3}	-45	-19.471	3.363	3.363	51.06	51.05	32.28	32.28
T_{-2}	-20.705	-19.471	10.34	10.35	56.24	56.24	110.21	110.23
T_{-1}	0	-19.471	31.87	31.87	46.55	46.54	99.03	99.02
T_0	20.705	-19.471	14.19	14.19	34.26	34.26	68.37	68.38
T_1	45	-19.471	37.83	37.83	46.33	46.34	86.81	86.83

^a $c/d=0.5$, $2H/d=0.5$, $\epsilon_+ = 1$, $\epsilon_- = 2.25$, $\mu_\pm = 1$, $\lambda/d=0.5$, $\theta=35.264^\circ$, $\phi=30^\circ$, $\delta=45^\circ$, and $\psi=90^\circ$. IM, present integral method; MM, Li's modal method [33].

^bDiffraction order.

Table 2. Diffraction Angles (θ , ϕ), Diffraction Efficiencies (η), and Polarization Angles (δ , ψ) of a Metallic Lamellar Grating^a

DO ^b	θ (IM), deg	ϕ (IM), deg	η (MM), %	η (IM), %	δ (MM), deg	δ (IM), deg	ψ (MM), deg	ψ (IM), deg
R_{-2}	-43.715	-20.705	7.31	7.52	62.48	61.85	52.74	48.30
R_{-1}	-9.007	-20.705	13.51	13.25	15.35	15.79	-12.05	-12.23
R_0	22.208	-20.705	42.99	44.27	41.25	41.33	171.21	170.15
R_1	65.852	-20.705	30.24	31.05	75.23	75.64	168.78	166.30

^a $c/d=0.5$, $2H/d=1$, $\epsilon_+=1$, $\epsilon_-=(-24.99, 1)$, $\mu_\pm=1$, $\lambda/d=0.5$, $\theta=22.208^\circ$, $\phi=20.705^\circ$, $\delta=45^\circ$, and $\psi=0$. IM, present integral method; MM, Li's modal method [33].

^bDiffraction order.

To examine the convergence of diffraction efficiencies, we choose as a sample the slanted (overhanging) lamellar highly conducting grating similar to that from Figs. 10 and 11 of [36], a rather difficult case, but for the refractive index $\nu_=(0, 100)$ instead of $\nu_=(0.01, 10)$ as in [36]. That means that we study an almost perfectly conducting non-function-profiled grating with a zero real part and a big imaginary part of the refractive index, using our solver for the finite conductivity, the case probably not possible

for many rigorous methods, even with all known improvements and artificial inclusions [36]. Note that, using the refractive index from the example of [36], the convergence rate of our solver is so high that no interesting data to discuss can be seen even for small values of N . So in Fig. 3 the convergence of the diffraction efficiencies with respect to the truncation parameter N under N doubling is demonstrated for $N_0=15$ and $K=9$ by using the much harder refractive index mentioned above. The efficiency values

Table 3. Diffraction Angles (θ , ϕ), Diffraction Efficiencies (η), and Polarization Angles (δ , ψ) of a Dielectric Sine Grating for $B_z=0^a$

DO ^b	θ (IM), deg	ϕ (IM), deg	η (CM), %	η (IM), %	δ (CM), deg	δ (IM), deg	ψ (CM), deg	ψ (IM), deg
R_{-3}	-43.384	-15	1.121	1.121	71.01	70.99	3.62	3.60
R_{-2}	-9.744	-15	3.741	3.741	26.91	26.90	0.93	0.93
R_{-1}	20.389	-15	3.873	3.873	63.25	63.25	178.16	178.18
R_0	60	-15	10.33	10.33	88.93	88.93	178.06	178.05
T_{-5}	-57.013	-7.435	0.01858	0.01855	80.18	80.19	-114.16	-114.68
T_{-4}	-35.921	-7.435	0.002466	0.002482	52.39	52.58	99.81	100.24
T_{-3}	-19.545	-7.435	0.7396	0.7394	57.62	57.61	-179.23	-179.28
T_{-2}	-4.729	-7.435	4.922	4.922	22.89	22.90	174.83	174.84
T_{-1}	9.770	-7.435	9.925	9.923	60.39	60.39	4.71	4.72
T_0	24.949	-7.435	7.146	7.145	77.33	77.32	6.83	6.84
T_1	42.371	-7.435	51.83	51.83	84.43	84.43	-5.77	-5.78
T_2	67.826	-7.435	6.351	6.351	84.85	84.85	-11.33	-11.39

^a $2H/d=0.3$, $\epsilon_+=1$, $\epsilon_-=-4$, $\mu_\pm=1$, $\lambda/d=0.5$, $\theta=60^\circ$, $\phi=15^\circ$, $\delta=81.501^\circ$, and $\psi=0$. IM, present integral method; CM, Li's coordinate transformation method [5].

^bDiffraction order.

Table 4. Diffraction Angles (θ , ϕ), Diffraction Efficiencies (η), and Polarization Angles (δ , ψ) of a Dielectric Sine Grating for $E_z=0^a$

DO ^b	θ (IM), deg	ϕ (IM), deg	η (CM), %	η (IM), %	δ (CM), deg	δ (IM), deg	ψ (CM), deg	ψ (IM), deg
R_{-3}	-43.384	-15	1.121	1.121	71.01	70.99	3.62	3.60
R_{-2}	-9.744	-15	3.741	3.741	26.91	26.90	0.93	0.93
R_{-1}	20.389	-15	3.873	3.873	63.25	63.25	178.16	178.18
R_0	60	-15	10.33	10.33	88.93	88.93	178.06	178.05
T_{-5}	-57.013	-7.435	0.01858	0.01855	80.18	80.19	-114.16	-114.68
T_{-4}	-35.921	-7.435	0.002466	0.002482	52.39	52.58	99.81	100.24
T_{-3}	-19.545	-7.435	0.7396	0.7394	57.62	57.61	-179.23	-179.28
T_{-2}	-4.729	-7.435	4.922	4.922	22.89	22.90	174.83	174.84
T_{-1}	9.770	-7.435	9.925	9.923	60.39	60.39	4.71	4.72
T_0	24.949	-7.435	7.146	7.145	77.33	77.32	6.83	6.84
T_1	42.371	-7.435	51.83	51.83	84.43	84.43	-5.77	-5.78
T_2	67.826	-7.435	6.351	6.351	84.85	84.85	-11.33	-11.39

^a $2H/d=0.3$, $\epsilon_+=1$, $\epsilon_-=-4$, $\mu_\pm=1$, $\lambda/d=0.5$, $\theta=60^\circ$, $\phi=15^\circ$, $\delta=8.499^\circ$, and $\psi=180^\circ$. IM, present integral method; CM, Li's coordinate transformation method [5].

^bDiffraction order.

Table 5. Diffraction Angles (θ , ϕ), Diffraction Efficiencies (η), and Polarization Angles (δ , ψ) of a Metallic Echelette Grating for $\delta=0^\alpha$

DO ^b	θ (IM), deg	ϕ (IM), deg	η (CM), %	η (IM), %	δ (CM), deg	δ (IM), deg	ψ (CM), deg	ψ (IM), deg
R_{-1}	-40.746	-40	12.99	12.97	39.409	39.447	-175.87	-175.93
R_0	0	-40	28.49	28.45	86.449	86.414	-51.16	-50.97
R_1	40.746	-40	24.77	24.81	39.237	39.209	7.58	7.67

^a $\zeta=30^\circ$, $\epsilon_+=1$, $\epsilon_-=(-45,28)$, $\mu_\pm=1$, $\lambda/d=0.5$, $\theta=0$, $\phi=40^\circ$, and $\psi=0$. IM, present integral method; CM, Li's coordinate transformation method [35].

^bDiffraction order.

stabilize, and the convergence is starting at $N=60$ and achieved with high accuracy at $N=960$. Note that $\Delta_{1920,8}=4.21 \times 10^{-4}$ and $\Delta_{3840,9}=1.50 \times 10^{-4}$, and the energy balance error is $\sim 10^{-4}$ for these values of N . Thus, the convergence rate is high enough, taking into account the difficult case tested. Moreover, because of solution peculiarities for profiles with edges, the convergence rate even is better for $\epsilon_-=(-10^5,0)$, but the calculation time is longer. The absorption calculated from Eq. (26) is very small for such a grating ($\sim 10^{-5}$), and its nonnegative magnitude and decreasing are also a good measure of the convergence and the calculation accuracy. One can also check of the absolute accuracy of calculation results for this example by using the perfect conductivity model. The asymptotic efficiency values calculated by using this model differ from those obtained by using the finite conductivity approach (0.9105 and 0.0894 for -1 and 0 orders, respectively) by not more than a few hundredths of a percent. The total computation time for all points presented in Fig. 3 is ~ 35 min on the above mentioned PC, and the required RAM is ~ 2 Gbytes. In this case the use of nongraded meshes and the numerical differentiation of V^+ gave the most accurate results compared with data obtained by applying other computational options.

The computation time T for the considered one-interface conical diffraction solver is essentially a function only of the number of unknowns, which is proportionally to N . The general dependence $T(N)$ of boundary integral equation formalisms is proportional to N^3 owing to a square dependence on N for the Green's functions and their derivatives calculations and the summation of these computed values that is proportional to N [17,23,24]. In addition, a direct linear equation solver requires a time that is also proportional to N^3 . To speed up the presented calculation solver two substantial accelerations have been used. The first one is Ewald's method for the kernel com-

putation; the second one is solving systems of linear equations iteratively. As a result, the computation time is proportional to N^2 , which is clearly seen in Fig. 4 for the typical example described in Table 2. If the iterative solver cannot give correct results after a prescribed number of iterations, then the direct solver is applied. Fortunately, this situation occurs in infrequent or hard cases only.

C. Efficiency of Grazing-Incidence Real-Groove-Profile Off-Plane Grating in X-Rays

Grazing-incidence off-plane gratings have been suggested for the International X-ray Observatory (IXO) [37]. Compared with gratings in the classical in-plane mount, x-ray gratings in the off-plane mount have the potential for superior resolution and efficiency for the IXO mission. The results of efficiency calculations for such a gold-blazed soft-x-ray grating in a conical mount using the groove profile derived from atomic force microscopy measurements are shown in Fig. 5. The average interface shape having 123 nodes is presented in Fig. 6. All grating and light parameters are listed in the figure caption. The incident beam in the rigorous calculations was assumed to be 81% TM polarized, which means the electric vectors of the incident wave and the diffracted waves are approximately parallel to the surface of the grating at the given diffraction angles. In Fig. 5 the numerical results of the presented IM for a finite boundary conductivity are compared with those based on the IM with the perfect boundary conductivity multiplied by Fresnel reflectances. The incident beam in the computations based on the perfect conductivity model was assumed to be 100% TE polarized ($B_z \approx 0$).

Rigorous computations carried out by the presented method show that for the considered grating model all the order efficiencies are not sensitive to a polarization state

Table 6. Diffraction Angles (θ , ϕ), Diffraction Efficiencies (η), and Polarization Angles (δ , ψ) of a Metallic Echelette Grating for $\delta=90^\alpha$

DO ^b	θ (IM), deg	ϕ (IM), deg	η (CM), %	η (IM), %	δ (CM), deg	δ (IM), deg	ψ (CM), deg	ψ (IM), deg
R_{-1}	-40.746	-40	53.15	53.15	54.0	54.0	13.31	13.37
R_0	0	-40	17.51	17.48	4.53	4.58	95.49	95.21
R_1	40.746	-40	9.423	9.444	49.47	49.41	-171.24	-171.22

^a $\zeta=30^\circ$, $\epsilon_+=1$, $\epsilon_-=(-45,28)$, $\mu_\pm=1$, $\lambda/d=0.5$, $\theta=0$, $\phi=40^\circ$, and $\psi=0$. IM, present integral method; CM Li's coordinate transformation method [35].

^bDiffraction order.

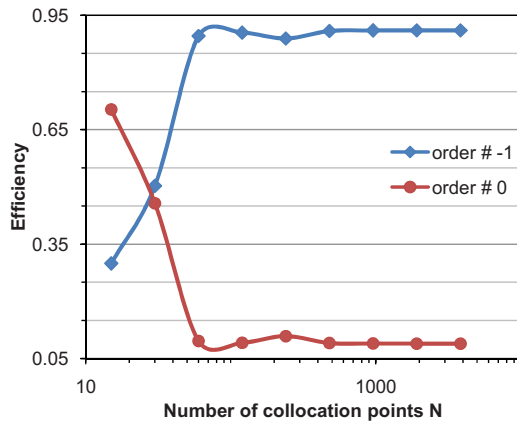


Fig. 3. (Color online) Diffraction efficiencies of a highly conducting grating with $c/d=0.5$ and $2H/d=0.3$, having the lamellar profiles slanted at an angle of 45° and hence being overhanging grooves, versus number of collocation points N . Other parameters are $\epsilon_+ = 1$, $\epsilon_- = (-10^4, 0)$, $\mu_\pm = 1$, $\lambda/d = 0.8$, $\theta = 26.565^\circ$, $\phi = 14.478^\circ$, $\delta = 0$, and $\psi = 0$.

and that efficiency jumps do not occur in the wavelength range investigated. For any polarization state order efficiencies differ from those presented in Fig. 5 by not more than a few tenths of a percent. In contrast, calculations based on the perfectly conducting boundary model are very sensitive to the polarization state, and sharp Rayleigh anomalies for the TM-polarized incident radiation occur. They were predicted earlier for such a grating using the in-plane boundary IM and the invariance theorem [39]. As can be seen in Fig. 5, the agreement between the data obtained by the finite conductivity model and the perfect conductivity model is good when TE-polarized incident radiation is used for the perfect conductivity model.

Here 800 collocation points, no mesh scaling, and the differentiation of V^+ have been used to calculate the finite-conducting real-groove-profile example that allocates a space of 144 Mbytes. The energy balance error calculated from Eq. (26) is $\sim 10^{-4}$ in the investigated wavelength range. The average computation time taken up by one wavelength on the above mentioned laptop is ~ 40 s. The time of a computation using the perfect conductivity model is about five times shorter at the same accuracy.

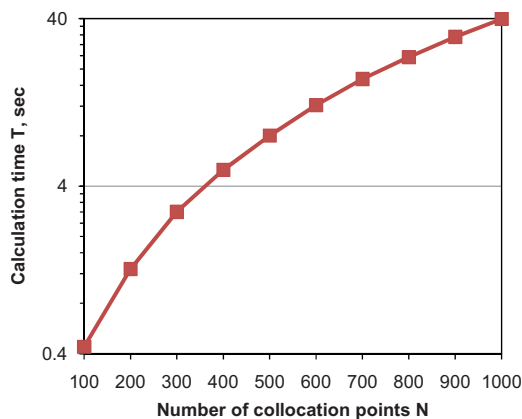


Fig. 4. (Color online) Computation time for the example described in Table 2.

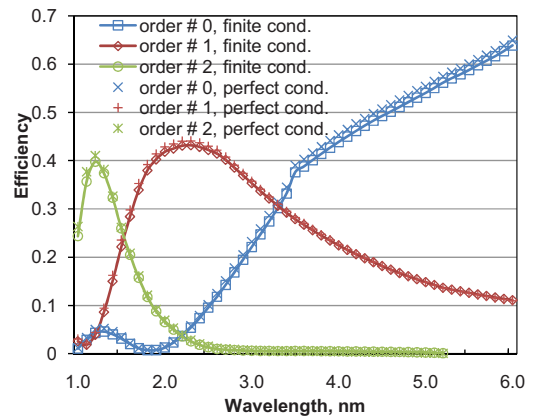


Fig. 5. (Color online) Diffraction efficiencies of a gold polygonal grating with 123 nodes, $\mu_\pm = 1$, and $d = 200$ nm for the incident wave with $\theta = -30^\circ$ and $\phi = 88^\circ$: finite conductivity model ($\delta = 34.143^\circ$ and $\psi = 0$) and perfect conductivity model ($B_z \approx 0$: $\delta = 30.015^\circ$ and $\psi = 180^\circ$) versus wavelength λ . Refractive indices of gold were taken from [38].

5. SUMMARY AND CONCLUSIONS

Off-plane scattering of time-harmonic plane waves by one-dimensional structures has been considered. The term “one-dimensional” refers to a general diffraction grating or a rough mirror having arbitrary conductivity on a planar surface in \mathbb{R}^3 , which is periodic in one surface direction, constant in the second, and has an arbitrary profile including edges and nonfunctions. The electromagnetic formulation of conical diffraction by gratings transformed to a system of two Helmholtz equations in \mathbb{R}^2 , which are coupled by jump conditions at the interfaces between different materials, was presented.

The integral equations for conical diffraction were obtained containing the boundary integrals of the single- and double-layer potentials, and the tangential derivative of single-layer potentials were interpreted as singular integrals. A full rigorous theoretical foundation of the conical boundary IM was established for the first time. Besides, we provided a formula for the direct calculation of the absorption of gratings in conical mounts. Some rules that are expedient for the numerical implementation of the described theory were presented.

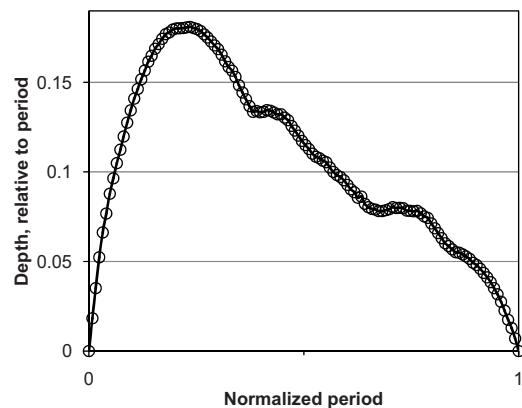


Fig. 6. Average groove profile measured by atomic force microscopy.

The results of efficiencies and polarization angles comparing with the data obtained by Li using the modal (lamellar profiles) and the coordinate transformation (sinus and echelette profiles) conical solvers for transmission and reflection gratings are in a good agreement. The high rate of convergence, the high accuracy, and the short computation time of the presented solver were demonstrated for various samples. An example of rigorous efficiency computations of the soft-x-ray grazing-incidence off-plane grating suggested for the IXO mission was demonstrated by using the 123-node border profile measured by atomic force microscopy and realistic refractive indices data.

The solver developed and tested is found to be accurate and efficient for solving conical diffraction problems, including difficult cases of high-conductive surfaces, borders with edges, real border profiles, and gratings working at very short wavelengths.

ACKNOWLEDGMENTS

The authors feel indebted to Lifeng Li (Tsinghua University, China) for the information provided and fruitful testing. Helpful discussions with Bernd Kleemann (Carl Zeiss AG, Germany), Andreas Rathsfeld (WIAS, Germany), and Sergey Sadov (New Foundland Memorial University, Canada) are greatly appreciated.

REFERENCES

1. P. Vincent, "Differential methods," in *Electromagnetic Theory of Gratings*, Vol. 22 of Topics in Current Physics, R. Petit, ed. (Springer, 1980), pp. 101–121.
2. M. Neviere and E. Popov, *Light Propagation in Periodic Media: Differential Theory and Design* (Marcel Dekker, 2002).
3. E. Popov and L. Mashev, "Conical diffraction mounting generalization of a rigorous differential method," *J. Opt.* **17**, 175–180 (1986).
4. S. J. Elston, G. P. Bryan-Brown, and J. R. Sambles, "Polarization conversion from diffraction gratings," *Phys. Rev. B* **44**, 6393–6400 (1991).
5. L. Li, "Multilayer coated diffraction gratings: differential method of Chandezon *et al.* revisited," *J. Opt. Soc. Am. A* **11**, 2816–2828 (1994).
6. J. P. Plumey, G. Granet, and J. Chandezon, "Differential covariant formalism for solving Maxwell's equations in curvilinear coordinates: oblique scattering from lossy periodic surfaces," *IEEE Trans. Antennas Propag.* **43**, 835–842 (1995).
7. L. Li, "Multilayer modal method for diffraction gratings of arbitrary profile, depth, and permittivity," *J. Opt. Soc. Am. A* **10**, 2581–2591 (1993).
8. F. Zolla and R. Petit, "Method of fictitious sources as applied to the electromagnetic diffraction of a plane wave by a grating in conical diffraction mounts," *J. Opt. Soc. Am. A* **13**, 796–802 (1996).
9. Ch. Hafner, *Post-modern Electromagnetics: Using Intelligent Maxwell Solvers* (Wiley, 1999).
10. J. Elschner, R. Hinder, and G. Schmidt, "Finite element solution of conical diffraction problems," *Adv. Comput. Math.* **16**, 139–156 (2002).
11. R. Köhle, "Rigorous simulation study of mask gratings at conical illumination," *Proc. SPIE* **6607**, 66072Z (2007).
12. L. Tsang, J. A. Kong, K.-H. Ding, and C. O. Ao, *Scattering of Electromagnetics Waves: Numerical Simulations* (Wiley, 2001), pp. 61–110.
13. D. W. Prather, M. S. Mirotznic, and J. N. Mait, "Boundary integral methods applied to the analysis of diffractive optical elements," *J. Opt. Soc. Am. A* **14**, 34–43 (1997).
14. J. M. Bendickson, E. N. Glytsis, and T. K. Gaylord, "Modeling considerations for rigorous boundary element method analysis of diffractive optical elements," *J. Opt. Soc. Am. A* **18**, 1495–1507 (2001).
15. E. G. Loewen and E. Popov, *Diffraction Gratings and Applications*, Vol. 58 of Optical Engineering Series (Marcel Dekker, 1997), pp. 367–399.
16. D. Maystre, M. Neviere, and R. Petit, "Experimental verifications and applications of the theory," in *Electromagnetic Theory of Gratings*, Vol. 22 of Topics in Current Physics, R. Petit, ed. (Springer, 1980), pp. 159–225.
17. L. I. Goray, I. G. Kuznetsov, S. Yu. Sadov, and D. A. Content, "Multilayer resonant subwavelength gratings: effects of waveguide modes and real groove profiles," *J. Opt. Soc. Am. A* **23**, 155–165 (2006).
18. B. H. Kleemann and J. Erxmeyer, "Independent electromagnetic optimization of the two coating thicknesses of a dielectric layer on the facets of an echelette grating in Littrow mount," *J. Mod. Opt.* **51**, 2093–2110 (2004).
19. M. Saillard and D. Maystre, "Scattering from metallic and dielectric surfaces," *J. Opt. Soc. Am. A* **7**, 982–990 (1990).
20. B. H. Kleemann, J. Gatzke, Ch. Jung, and B. Nelles, "Design and efficiency characterization of diffraction gratings for applications in synchrotron monochromators by electromagnetic methods and its comparison with measurement," *Proc. SPIE* **3150**, 137–147 (1997).
21. L. I. Goray and J. F. Seely, "Efficiencies of master replica, and multilayer gratings for the soft-x-ray-extreme-ultraviolet range: modeling based on the modified integral method and comparisons with measurements," *Appl. Opt.* **41**, 1434–1445 (2002).
22. A. Rathsfeld, G. Schmidt, and B. H. Kleemann, "On a fast integral equation method for diffraction gratings," *Comm. Comp. Phys.* **1**, 984–1009 (2006).
23. D. Maystre, "Integral methods," in *Electromagnetic Theory of Gratings*, Vol. 22 of Topics in Current Physics, R. Petit, ed. (Springer, 1980), pp. 53–100.
24. A. Pomp, "The integral method for coated gratings: computational cost," *J. Mod. Opt.* **38**, 109–120 (1991).
25. B. Kleemann, A. Mitreiter, and F. Wyrowski, "Integral equation method with parametrization of grating profile. Theory and experiments," *J. Mod. Opt.* **43**, 1323–1349 (1996).
26. E. Popov, B. Bozhkov, D. Maystre, and J. Hoose, "Integral method for echelles covered with lossless or absorbing thin dielectric layers," *Appl. Opt.* **38**, 47–55 (1999).
27. L. I. Goray, "Modified integral method for weak convergence problems of light scattering on relief grating," *Proc. SPIE* **4291**, 1–12 (2001).
28. L. I. Goray and S. Yu. Sadov, "Numerical modeling of coated gratings in sensitive cases," in *Diffractive Optics and Micro-Optics*, R. Magnusson, ed., Vol. 75 of OSA Trends in Optics and Photonics Series (Optical Society of America, 2002), 365–379.
29. L. I. Goray, J. F. Seely, and S. Yu. Sadov, "Spectral separation of the efficiencies of the inside and outside orders of soft-x-ray-extreme ultraviolet gratings at near normal incidence," *J. Appl. Phys.* **100**, 094901 (2006).
30. L. I. Goray, "Specular and diffuse scattering from random asperities of any profile using the rigorous method for x-rays and neutrons," *Proc. SPIE* **7390-30**, 73900V (2009).
31. J. Elschner, R. Hinder, F. Penzel, and G. Schmidt, "Existence, uniqueness and regularity for solutions of the conical diffraction problem," *Math. Models Meth. Appl. Sci.* **10**, 317–341 (2000).
32. G. Schmidt, "Boundary integral methods for periodic scattering problems," in *Around the Research of Vladimir Maz'ya II. Partial Differential Equations* (Springer, 2010), pp. 337–364.
33. L. Li, "A modal analysis of lamellar diffraction gratings in conical mountings," *J. Mod. Opt.* **40**, 553–573 (1993).
34. M. Mansuripur, L. Li, and W.-H. Yeh, "Diffraction gratings: part 2," *Opt. Photonics News* **10**, August 1, 1999, pp. 44–48.

35. L. Li and J. Chandezon, "Improvement of the coordinate transformation method for surface-relief gratings with sharp edges," *J. Opt. Soc. Am. A* **13**, 2247–2255 (1996).
36. E. Popov, B. Chernov, M. Neviere, and N. Bonod, "Differential theory: application to highly conducting gratings," *J. Opt. Soc. Am. A* **21**, 199–206 (2004).
37. "IXO International X-ray observatory," Goddard Space Flight Center, <http://ixo.gsfc.nasa.gov/technology/xgs.html>.
38. "X-ray interactions with matter," http://henke.lbl.gov/optical_constants/.
39. J. F. Seely, L. I. Goray, B. Kjornrattanawanich, J. M. Laming, G. E. Holland, K. A. Flanagan, R. K. Heilmann, C.-H. Chang, M. L. Schattenburg, and A. P. Rasmussen, "Efficiency of a grazing-incidence off-plane grating in the soft-x-ray region," *Appl. Opt.* **45**, 1680–1687 (2006).